Mathematical Modeling of Intracellular Calcium in Presence of Receptor: A Homeostatic Model for Endothelial Cell

Ananta Kumar, Zhe Gou, Sovan Lal Das, Abdul I Barakat, Chaouqi Misbah

Mathematical Modeling of Intracellular Calcium in Presence of Receptor: A Homeostatic Model for Endothelial Cell

Ananta Kumar Nayak[1], Zhe Gou[1], Sovan Lal Das[2], Abdul I. Barakat[3] and Chaouqi Misbah[1*]

[1]Université Grenoble Alpes, CNRS, LIPhy, Grenoble, 38000, France.
[2]Indian Institute of Technology Palakkad, Palakkad, 678557, Kerala, India.
[3]LadHyX, CNRS, Ecole polytechnique, Institut polytechnique de Paris, Palaiseau, 91120, France.

*Corresponding author(s). E-mail(s): chaouqi.misbah@univ-grenoble-alpes.fr;

Abstract

Calcium is a ubiquitous molecule and second messenger that regulates many cellular functions ranging from exocytosis to cell proliferation at different time scales. In the vasculature, a constant adenosine triphosphate (ATP) concentration is maintained because of ATP released by red blood cells (RBCs). These ATP molecules continuously react with purinergic receptors on the surface of endothelial cells (ECs). Consequently, a cascade of chemical reactions are triggered that result in a transient cytoplasmic calcium (Ca^{2+}), followed by return to its basal concentration. The mathematical models proposed in literature are able to reproduce the transient peak. However, the trailing concentration is always higher than the basal cytoplasmic Ca^{2+} concentrations, and the Ca^{2+} concentration in endoplasmic reticulum (ER) remains lower than its initial concentration. This means that the intracellular homeostasis is not recovered. We propose, herein, a minimal model of calcium kinetics. We find that the desensitization of EC surface receptors due to phosphorylation and recycling plays a vital role in maintaining calcium homeostasis in the presence of a constant stimulus (ATP). The model is able to capture several experimental observations such as refilling of Ca^{2+} in the ER, variation of cytoplasmic Ca^{2+} transient peak in ECs, the resting cytoplasmic Ca^{2+} concentration, the effect of removing ATP from the plasma on Ca^{2+} homeostasis, and the saturation of cytoplasmic Ca^{2+} transient peak with increase in ATP concentration. Direct confrontation with several experimental results is conducted.This work paves the way to systematic studies for coupling between blood flow and chemical signaling, and should contribute to a better understanding of the relation between (patho)physiological conditions and Ca^{2+} kinetics.

Keywords: homeostasis; desensitization; ATP; RBCs; phosphorylation; recycling

1 Introduction

Ca^{2+} is a ubiquitous ion and second messenger that regulates many cellular functions ranging from exocytosis to cell proliferation occurring on different time scales [1]. Ca^{2+} is known to directly regulate several proteins, thereby implicitly controlling many cellular functions such as gene transcription, fertilization, and arterial vasodilation [1]. The sudden rise in cytoplasmic Ca^{2+} occurs due to the release of intracellular stored Ca^{2+} from the endoplasmic reticulum (ER), which

accounts for 75% of the intracellular stored Ca^{2+} concentration [2]. Ca^{2+} is released from the ER due to the action of inositol 1,4,5-trisphosphate (IP_3) on inositol trisphosphate receptors (IP_3R) present on the ER membrane. This is preceded by a sequence of events in the plasma membrane (PM) in order to transduce the extracellular information to the second messenger IP_3.

We are interested here in intracellular Ca^{2+} dynamics in endothelial cells (ECs), which form the inner lining of all blood vessels. Ca^{2+} release from the ER of ECs may be triggered by different stimuli including shear stress [3], hormones [4], and extracellular adenosine triphosphate (ATP) [5]. The effect of ATP released by red blood cells (RBCs) on intracellular Ca^{2+} generation is particularly important because of ATP's crucial role in regulating blood flow and vascular tone [6]. RBCs release ATP under shear stress and cell deformation. ATP released by RBCs reacts with purinergic EC receptors ($P2Y_2$) (a class of membrane receptors that mediates vascular reactivity) to elicit the calcium reaction cascade in ECs. Subsequently, ECs release vasodilators such as nitric oxide (NO), which maintains vascular tone by countering the effects of endothelium-derived vasoconstrictors, such as endothelin and angiotensin-II [7]. In addition, NO inhibits platelet adherence and aggregation, proliferation of vascular smooth muscle cells (VSMC), and leukocyte adhesion and infiltration. Thus, understanding EC Ca^{2+} kinetics is of major interest.

There is a general consensus that the calcium pathway involves three main steps: (i) reaction of a ligand with a receptor on the EC surface, (ii) generation of IP_3 due to ligand-receptor binding, and (iii) IP_3-induced channel opening on the ER membrane to release calcium from internal stores into the cytoplasm. The three main variables are thus (besides ATP) IP_3 concentration, store calcium concentration, and and cytoplasmic calcium concentration, denoted, respectively, by $IP_3(t)$, $Ca_s(t)$, $Ca_c(t)$, which are all time-dependent variables. Several models are available that take into account the kinetics of these three quantities [8–15]. These models have successfully accounted for several experimental features, such as cytoplasmic Ca^{2+} peak amplitude, duration of peak, and the elevated resting Ca^{2+} concentration from its initial concentration. Additionally, some of these models have introduced several new variables into the model such as cytoplasmic Ca^{2+}-calmodulin(CaM)-activated endothelial nitric oxide synthase (eNOS) [12, 14] and transmembrane potential [13] across the PM. The authors in Refs. [12, 14] have further extended their model to include inhomogeneous distribution of ATP due to advection and diffusion and have suggested that atherosclerosis development is highly dependent on cytoplasmic Ca^{2+} concentration.

A main question is how do ECs manage to achieve intracellular homeostasis in the presence of ATP in the bloodstream. The concentration of ATP in blood plasma is maintained typically at a value of a few μM. This would mean that ECs are constantly in contact with ATP with different local ATP concentration, meaning that IP_3 would be constantly activated, not enabling the ER to be fully refilled by calcium. In addition, experiments have shown [5] that ECs produce a single calcium peak in the presence of ATP. When ATP is removed after the calcium response from the plasma and then reintroduced after a few minutes later, no calcium cellular response was observed; a response is only observed after a certain period of time (about 20 minutes is allowed to elapse). However, the same EC responds to a different agonist, histamine, immediately. This clearly highlights the fact of desensitization or inactivity of membrane receptors to ATP for a period of time. It is worthwhile to bring attention that most of ECs in that experiment responded to ATP (1-500 μM concentrations) with a single transient peak before returning to resting Ca^{2+} concentration. Moreover, in the same experiment, a few number of ECs have complex oscillations as well as transient peak with elevated resting Ca^{2+} concentration.

In literature[8, 16–24], most of Ca^{2+} models have been developed to understand the mechanism behind the cytoplasmic Ca^{2+} oscillations to agonists in various cells. These Ca^{2+} oscillations are generated due to two main pathways (i) the participation of cytoplasmic Ca^{2+} in activating or deactivating the IP_3R channels in the presence of constant IP_3 concentration (ii) Ca^{2+}-induced IP_3 generation and degradation due to positive or negative effects of rising cytoplasmic Ca^{2+} concentration. Furthermore, certainly, another way of possible Ca^{2+} oscillation is due to the phosphorylation and dephosphorylation of surface

receptors by the protein kinase C (PKC), which is either activated due to the rising of diacylglycerol (DAG) concentration [25] or both DAG and cytoplasmic Ca^{2+} [26, 27] concentrations. Thus, the essential ingredients in these models to have oscillation must contain at least a downstream positive or negative feedback pathway which could affect the upstream biochemical reactions. Additionally, these models can be considered as a homeostatic model if all primary variables oscillate about their resting concentrations.

Calcium evolution in time is not always oscillatory in nature. For example, in in most ECs a single calcium peak is observed in the presence of agonist (e.g. ATP) [5]. Several attempts [9, 11, 13] have been made to understand the occurrence of a single peak of Ca^{2+}. Because of the strategic location of ECs in vascular wall and its functions to maintain vascular homeostasis, the modeling of Ca^{2+} in ECs require much more attentions to understand the detail kinetics of the Ca^{2+} dynamics. Several attempts have been made in past years to develop and understand the single peak cytoplasmic Ca^{2+} dynamics without including the surface receptor dynamics into their model [9, 11, 13]. These models have basically been focused on the cytoplasmic Ca^{2+} peak as observed in experiments, and able to reproduce the homeostasis only in the absence of agonist concentration, but not when agonist is not removed. However, when these models are tested in the presence of agonists, a major deviation from post-response homeostatic conditions is revealed for cytoplasmic Ca^{2+}, as well as for store Ca^{2+}, and IP_3. These facts, as well as the above experimental observations according to which cells do not respond to agonists after their immediate reintroduction [5] may point to the fact that membrane receptors activation/deactivation can play a significant role. Along this line some authors [29] proposed a detailed ligand-activated receptor dynamics model in which they considered a closed cell model. This model was able to produce a robust transient peak. However, the post-response plateau of Ca^{2+} is found to be higher that the resting Ca^{2+} concentration (i.e., lack of homeostasis). This is due to positive feedback of cytoplasmic Ca^{2+} on IP_3 generation (see below). In addition, this model considered some simplifications (i) a closed cell model was adopted, meaning that there is no exchange with the external environment. However, the refilling of store Ca^{2+} [30, 31] must be achieved thanks to Ca^{2+} coming from the extracellular environment (ii) the phosphorylated receptors, free surface receptors which are phosphorylated due to the binding of ligands, were unable to recycle to free receptors when the ligands were washed out from the plasma. It is noteworthy to mention that we are exclusively aimed to develop a robust single Ca^{2+} peak homeostatic model.

Another model [26] also took into account the phosphorylation and dephosphorylation of G-proteins and free surface receptors (due to the negative feedback from the PKC enzyme activated by the action of both DAG and cytoplasmic calcium). The results obtained from this model, after mimicking agonist washing out from the plasma, are as follows: (i) the Ca^{2+} response from the cell was immediate with the same magnitude when the ligands were reintroduced again just after the occurrence of the calcium peak (1 to 50 seconds). This differs from experimental observations showing that a cell takes a minimum of 5 minutes to several hours to express a full response [5, 32] (ii) the number of free receptors do not reach initial concentration (concentrations of free receptors prior to ligands application) even after a quite long simulation time. We expect that under physiological conditions the phosphorylated receptors must be recycled to their initial concentration when ligands are removed from the plasma. Inspired by these models, we propose a further development in order identify how recycling of receptors can be incorporated, and how a time delay of cell response, after reintroducing agonist just after calcium peak, can be modeled. Our improved version is able to provide answers in favor of the above experimental facts. We will make several direct comparisons with experimental results, showing a reasonably good agreement with the proposed model.

2 Method and Model Development

2.1 Main ingredients of the model

In this section, we will develop a minimal single EC Ca^{2+} dynamics model capable of reproducing several experimental results. A major issue accounted for this model is how an ECs can maintain Ca^{2+} homeostasis in the presence of a constant ATP supply. Since ATP is constantly released by RBCs in blood, the EC might be expected to continuously produce cytoplasmic Ca^{2+} in response to this agonist. At the same time, the EC is expected to restore intracellular Ca^{2+} homeostasis in order to protect its organelles from the toxic effects of an elevated cytoplasmic Ca^{2+} concentration. Indeed, the EC develops a protective mechanism by phosphorylating ATP-bound receptors, which means that these receptors are no longer able to activate G-proteins, which are membrane ATP sensors. This thus leads to a decline in IP_3 generation, allowing the EC to restore intracellular homeostasis. Inspired by the study of [29] on receptor kinetics, we develop a modified version to study membrane receptor dynamics. When coupled to Ca^{2+} and IP_3 dynamics, this model accounts for several documented responses of ECs to ligands such as ATP.

2.2 G-protein cascade

The first stage of calcium generation starts with the ATP reacting with the so-called purinergic (designated as $P2Y_2$, see Figure 1) receptors on the EC surface. This elicits a cascade of reactions. A key player is the G-protein ($P2Y_2$ is a G-protein-coupled receptor), which transmits the signal from the outside to the inside of the EC. G-proteins are deactivated due to the hydrolysis of guanosine triphosphate (GTP) into guanosine diphosphate (GDP). So, the rate of change of G-protein concentration can be expressed as,

$$\frac{d[G]}{dt} = k_a\left(\delta + \rho_r\right)\left([G_t] - [G]\right) - k_d[G]\,, \qquad (1)$$

where $[x]$ represents the concentration of a chemical species x and k_a and k_d are the G-protein activation and deactivation rate constants, respectively. The ligand (ATP) concentration is denoted as $[L]$ and that of free receptors is denoted by $[R]$. Once ATP reacts with receptors, it gives rise to the LR complex whose concentration is denoted as $[LR]$. $[G_t]$ is the total concentration of G-protein molecules, and δ is the G-protein intrinsic activity parameter, i.e., R can independently activate G-proteins without binding to ligands. It is reported in several experiments that G-protein is able to sense and transduce shear stress-induced signals to the cytoplasm [56, 57]. This explains the reason behind a non-zero basal IP_3 concentration in the cytoplasm as reported by [33] and [34] in the absence of ligands (ATP); see below. It is important to stress that the ATP produced by ECs due to shear stress could contribute to basal IP_3 concentration. This formation of IP_3 is possible only when ATP molecules bind with free receptors. The investigation of mechanisms that play a significant role in maintaining the basal IP_3 concentration still remains an open area. Further experiments would be needed in order to better clarify this issue. Moreover, there is no quantitative data in literature reporting on the amount of ATP released at basal shear stress. It can be perceived from the works in [56, 57] that the shear induced basal IP_3 plays a vital role in maintaining basal IP_3 concentration without association of ligand-receptor. The ratio of receptors bound to ligands to the total number of $P2Y_2$ receptors is ρ_r (which will be related to receptor and ligand concentration; see Subsection 2.4 for more details). This is for the moment viewed as a constant before including below the receptor dynamics into the model. We can simplify Equation 1 by assuming that $[G]$ activation and deactivation is governed by fast kinetics [35], so that

$$[G] = [G_t]\frac{\rho_r + \delta}{\rho_r + \delta + K_g} \equiv [G_t]\lambda\,. \qquad (2)$$

where $K_g = k_d/k_a$ and $\lambda = \frac{\rho_r+\delta}{\rho_r+\delta+K_g}$

A remark is in order. Due to difference in the time scale of G-protein activation and deactivation, this approximation overestimates the IP_3 peak (see supplementary information, Figure S2). However, the trend remains similar to the results of the full model, i.e. without adiabatic elimination of G protein kinetics. This lends support to the fact the adiabatic elimination is reasonable. Additionally, GTP bound G-protein activates the PLC-enzyme, which then forms the IP_3 molecules

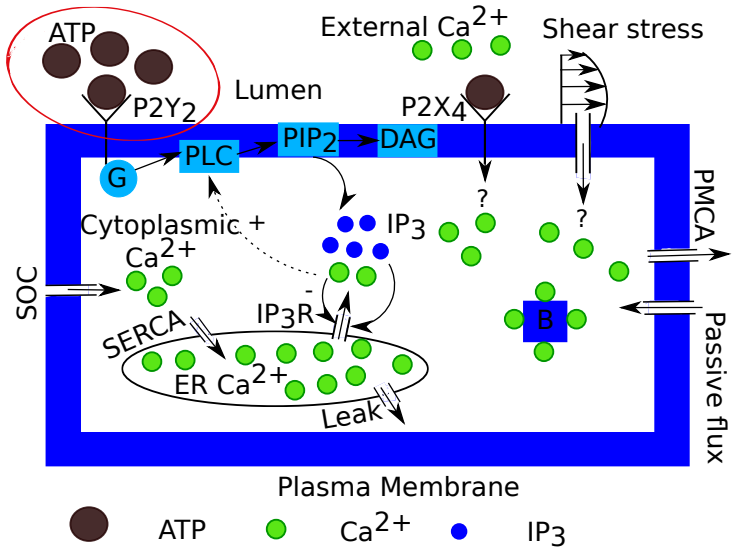

Fig. 1 Schematic of the Ca^{2+} homeostasis in the EC, where the abbreviations are, ATP: adensoine triphosphate, G: G-protein, PLC: phospholipase-C, PIP_2: phosphatidylinositol 4,5-bisphosphate, DAG: diacylglycerol, IP_3: 1,4,5-trisphosphate, IP_3R: 1,4,5-trisphosphate receptor, SOC: store-operated channel, SERCA: sarco/endoplasmic reticulum Ca^{2+}-ATPase, PMCA: plasma membrane Ca^{2+}-ATPase, B: buffer proteins. Question marks (?) refer the influx of extracellular Ca^{2+} into the cytoplasm due to the action of ATP on $P2X_4$ channel and shear stresses due to blood flow are not fully understood in experiments.

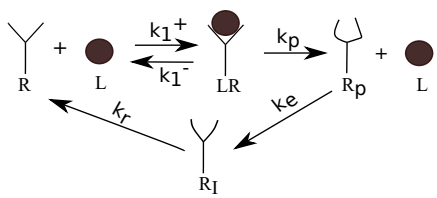

Fig. 2 The red color enclosure in Figure 1 represents the receptor and ligand binding dynamics. Free receptor, R, binds with a ligand, L, reversibly and forms a ligand-receptor complex, LR. This complex is irreversibly converted into the phosphorylated receptor, R_p and ligand, L and eventually, R_p converts into internalized receptor, R_I and then R.

by splitting PIP_2 molecules. The rate of change of IP_3 concentration, $[IP_3]$, can be defined as,

$$\frac{d\,[IP_3]}{dt} = q_{\text{gen}} - q_{\text{deg}}\,, \tag{3}$$

where q_{gen} and q_{deg} are the IP_3 generation and degradation fluxes, respectively, which are defined below. There is a positive feedback from Ca^{2+} released from the ER, which triggers an increase in IP_3 formation [8], so that

$$q_{\text{gen}} = \gamma\lambda\frac{[Ca_c]}{K_1 + [Ca_c]}\,, \tag{4}$$

with $\gamma = \alpha[G_t][(PIP_2)_t]/(N_A V_{\text{EC}})$, where, the denominator containing the product of N_A and V_{EC} allows to convert IP_3 generation in molar (M or mole/ltr). The entire cascade of reactions starting from G-protein activation to IP_3 generation is lumped into a single flux term given by Equation 4. The effective signal gain parameter is α, N_A is Avogadro number, V_{EC} is the EC volume, and $[(PIP_2)_t]$ is the total number of phosphatidylinositol 4,5-bisphosphate (PIP_2) molecules. We here assume that there is no change in the concentration of PIP_2 molecules, i.e., splitting and replenishing of PIP_2 molecules is regulated by fast reactions [35]. This means that the effect of G-proteins and $[(PIP_2)_t]$ enters as an effective multiplicative coefficient in this flux (in γ). The dissociation constant between the Ca^{2+} and PLC-enzyme is K_1 and is considered as an important parameter for the cytoplasmic Ca^{2+} oscillations

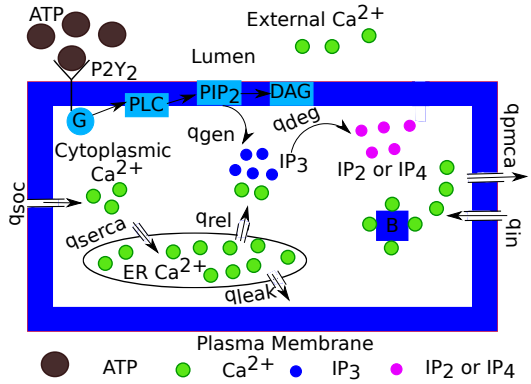

Fig. 3 Intracellular fluxes across the plasma and ER membranes. Detailed definitions of these fluxes are given in the text.

[8]. It turns out that keeping $K_1 \neq 0$ for ECs (single peak model) precludes return to homeostasis. Based on this observation, we will in the following set $K_1 = 0$. $[Ca_c]$ is the cytoplasmic Ca^{2+} concentration. The rate of IP_3 degradation due to the formation of IP_2 or IP_4 by kinases or phosphatases is given by

$$q_{\text{deg}} = k_2 \, [IP_3] \; . \tag{5}$$

where k_2 is the IP_3 degradation rate.

2.3 Intracellular calcium

The cytoplasm of an EC is a highly complex structure due to the complex shape of organelles and their arrangement with in the cytoplasm. The governing equation for the cytoplasmic Ca^{2+} concentration, $[Ca_c]$, is obtained by balancing the fluxes across the PM and ER membrane as shown in Figure 3 and is given by [11]

$$\frac{d\,[Ca_c]}{dt} = \beta \left(q_{\text{rel}} - q_{\text{serca}} + q_{\text{leak}} + q_{\text{soc}} + q_{\text{in}} - q_{\text{pmca}} \right) \; , \tag{6}$$

where β is defined as a buffer factor for immobile buffer proteins only. The expression for β is obtained by assuming that the reaction between the buffer proteins and cytoplasmic Ca^{2+} is faster than the Ca^{2+} flux rates across the PM and ER membranes (detailed derivation and justification are given in supplementary information). Therefore, following [36], we derive the expression for β as

$$\beta = \left\{ 1 + \frac{[B_t] \, \frac{k_7}{k_6}}{\left(\frac{k_7}{k_6} + [Ca_c] \right)^2} \right\}^{-1} \; . \tag{7}$$

where k_6 and k_7 are the association and dissociation rates between the buffer proteins and cytoplasmic Ca^{2+}, and $[B_t]$ is the total buffer protein concentration, a constant.

The fluxes q_{rel}, q_{serca}, q_{leak}, q_{soc}, q_{in}, and q_{pmca} used in Equation 6 are, respectively, the rates of change in the cytoplasmic Ca^{2+} concentration due to release through the IP_3R, uptake from the ER, a passive leak from the ER, ER-depleted influx from the extracellular space, a passive influx from the extracellular space, and efflux by the PM pump. The individual expressions for these fluxes are defined below. However, the expression for q_{in} is given in subsection 2.6, and is physically interpreted as the Ca^{2+} influx required to maintain Ca^{2+} homeostasis in the absence of ATP. The IP_3-induced Ca^{2+} releasing from the ER is defined as

$$q_{\text{rel}} = k_3 \frac{[IP_3]^3}{K_2^3 + [IP_3]^3} \frac{K_{i,Ca_c}^3}{[Ca_c]^3 + K_{i,Ca_c}^3} Ca_s \; , \tag{8}$$

where k_3 is the Ca^{2+} release rate from the ER, and K_2 is the IP_3 concentration at which half of the IP_3R sites are occupied by IP_3 molecules; K_{i,Ca_c} is the cytoplasmic Ca^{2+} for half-maximal inhibition of IP_3R, and $[Ca_s]$ is the ER Ca^{2+} concentration. Equation 8 states that the Ca^{2+} release rate from the ER is due to binding of three IP_3 molecules to the IP_3R. Moreover, several physiological IP_3R models are available in the literature in which both positive and negative effects of the cytoplasmic Ca^{2+}, i.e., calcium-induced-calcium-release (CICR) and calcium-induced-calcium-inhibition on IP_3R activation, are considered (for details see [37]). However, here we have only considered the latter because the effects of the former are not found in vascular ECs as modeled in [13]. In particular, we assume that the opening and closing of IP_3R channels are instantaneous. The Ca^{2+} uptake rate from the cytoplasm into the ER is defined by

$$q_{\text{serca}} = k_4 \frac{[Ca_c]^2}{K_3^2 + [Ca_c]^2} \; , \tag{9}$$

where k_4 is the Ca^{2+} uptake rate by sarco/endoplasmic reticulum Ca^{2+}-ATPase (SERCA) and K_3 is the Michaelis-Menten constant. The SERCA pumps cytoplasmic Ca^{2+} into the ER by using energy from ATP. The rate of passive leak of Ca^{2+} from the ER is assumed to be due to the defects in the ER membrane or may be due to the fixed capacity of ER.

$$q_{\text{leak}} = k_5[Ca_s]\,, \tag{10}$$

where k_5 is the Ca^{2+} leak rate from the ER. The linear dependence on $[Ca_s]$ have been verified to not be a limitation (taking for example a quadratic form, as in [11], leaves our results practically unchanged; the k_5 value will have a different dimension for the linear model adopted here; see Table 1).

In [31], it has been reported that a channel is only activated when the ER Ca^{2+} concentration gets depleted due to IP_3-dependent Ca^{2+} release from the ER and is termed store-operated calcium (SOC). SOC is considered one of the important channels for ER Ca^{2+} replenishment, allowing the extracellular Ca^{2+} flux into the cytoplasm. The mechanism of SOC activation is now well understood. Due to the depletion of the ER Ca^{2+}, a pathway is formed because of the interaction between the stromal interaction molecules (STIMs) and ORAIs in the ER and plasma membrane, respectively [37]. It is noteworthy to mention that these channels are switched off, STIMs and ORAIs get separated *i.e.*, calcium influx is zero, when the store is completely refilled with Ca^{2+} [30, 38]. We will see that this model reproduces the Ca^{2+} homeostasis both in the presence and absence of IP_3. Thus, the rate of change of the cytoplasmic Ca^{2+} due to the SOC is written as [39]

$$q_{\text{soc}} = k_{\text{soc}} \frac{1}{\left(1+\frac{[Ca_s]}{K_{\text{soc}}}\right)^n} \left([Ca_{\text{ex}}]-[Ca_c]\right) \left([Ca_s]\,(0)-[Ca_s]\right)\,, \tag{11}$$

where n is a constant, k_{soc} is the maximal Ca^{2+} influx rate through the SOC, and K_{soc} is the ER Ca^{2+} for the half-activation of the SOC. $[Ca_{\text{ex}}]$ and $[Ca_s]\,(0)$ are the external and initial ER Ca^{2+} concentrations (the homeostatic one), respectively. Equation **??** includes three important experimental observations: (1) the probability of SOC opening, (2) the fact that the amount of Ca^{2+} influx depends on the concentration gradient across the PM, and (3) the observation of no Ca^{2+} influx at resting conditions. The proposed model for SOC [39] was modified by adding the last term in Equation **??** to satisfy the third observation. q_{in} is the passive influx of Ca^{2+} due to defects in the PM, a constant whose expression is obtained in subsection 2.6 by satisfying the EC homeostasis condition. Note that because $[Ca_{\text{ex}}] \gg [Ca_c]$ under physiological conditions, in what follows we will make the approximation that $[Ca_{\text{ex}}]-[Ca_c] \simeq [Ca_{\text{ex}}]$.

The cytoplasmic Ca^{2+} efflux rate from the cytoplasm into the extracellular space is defined as

$$q_{\text{pmca}} = k_8 \frac{[Ca_c]^2}{K_4^2+[Ca_c]^2}\,, \tag{12}$$

where k_8 is the maximal Ca^{2+} efflux rate through plasma membrane Ca^{2+}-ATPase (PMCA), and K_4 is the cytoplasmic Ca^{2+} concentration for the half-sites of PMCA. Note that the second power of $[Ca_c]$ is used in Equations 9 and 12 because both of these pumps transfer two Ca^{2+} ions from the cytoplasm to the ER and extracellular space, respectively, by consuming one ATP.

Similarly, the rate of change of Ca^{2+} in the ER, $[Ca_s]$, is obtained by balancing the fluxes across the ER membrane, namely

$$\frac{d\,[Ca_s]}{dt} = v_r\left(q_{\text{serca}} - q_{\text{rel}} - q_{\text{leak}}\right)\,, \tag{13}$$

where v_r is a volume scaling factor, i.e., the ratio between the cytoplasm and the ER volumes. Note that the three fluxes appearing above are the same fluxes that appear in Equation 6. This results simply from mass conservation (exchange between ER and the rest of cytoplasm).

2.4 Receptor dynamics

When solving Equations 3, 6, and 13 (by using the different fluxes introduced above) for a constant value of ρ_r, we obtained similar results for calcium pulses as in [11] and other similar model [15] (see Figure S1 in supplementary information). One

important point is that the final steady state concentration of IP_3, cytoplasmic and ER Ca^{2+} turn out to be significantly different from their physiological concentration. In particular, the ER is not refilled, and IP_3 remains at a significantly higher level than its initial value (see Figure S1 in supplementary information). In principle, one expects physiological systems to ensure homeostasis, i.e., different concentrations ultimately revert to their initial values before the application of a stimulus. By taking into account receptor dynamics, we can propose a model that can capture the essential expected physiological response of calcium kinetics. The model is based on the observation that receptors R exist in 4 different states: (i) unbound receptor, R, (ii) bound receptor, LR (ligand-receptor complex), (iii) phosphorylated receptor, R_p, and (iv) internalized receptor, R_I as shown in Figure 2 [29]. One important assumption here is that phosphorylated receptors are no longer able to respond to the external ligands. Moreover, it is worthwhile to mention that the increase in phosphorylated receptor concentration leads to reduction in IP_3 generation, thereby the release of Ca^{2+} from the ER. However, the actual reason for receptor phosphorylation (or desensitization) is still poorly understood. The rate of change of the total unphosphorylated receptor concentration, $[R_s] = [R] + [LR]$ becomes (this is derived using the fast kinetics approach),

$$\frac{d[R_s]}{dt} = k_r[R_t] - \left(k_r + k_p \frac{[L]}{K_r + [L]}\right)[R_s] - k_r[R_p]\,, \tag{14}$$

where $[R_t] = [R_s] + [R_p] + [R_I]$ is the total receptor concentration. The terms proportional to k_r sum up to $k_r[R_I]$, implying that the internalized receptor can be recycled into membrane receptors (R or LR). We have summed up $[R]$ and $[LR]$ into a single term, $[R_s]$, owing to the fact that these two unphosphorylated receptors are responsible for the activation of G-proteins and subsequently the formation of IP_3 molecules. k_r and k_p are the rate constants at which R_I is recycled to R and LR phosphorylated to R_p, respectively. $K_r = k_1^-/k_1^+$ is the unphosphorylated receptor dissociation constant, where k_1^- and k_1^+ are respectively the forward and backward constants for the reversible reaction between L and R. Similarly, using the law of mass action, we can deduce the equation for the rate of change of the phosphorylated receptor concentration, $[R_p]$, i.e.,

$$\frac{d[R_p]}{dt} = k_p \frac{[L][R_s]}{K_r + [L]} - k_e[R_p]\,. \tag{15}$$

This model is inspired by that of Lemon et al. [29], which we have enriched by the fact that phosphorylated receptors R_p are converted into R in the absence of L. For that purpose, we have assumed that LR is irreversibly phosphorylated into R_p and subsequently R_p is internalized and recycled to R at rates k_e and k_r. This fact is witnessed in the second term of Equation 15, i.e., in the absence of ligand, $[L] = 0$, the rate of change of unphosphorylated receptor, R_p, is only dependent on the second term.

In subsection 2.2, we have assumed that ρ_r is a constant because we have implicitly assumed that the concentration of LR remains constant. When taking into account desensitization, the concentration of LR is no longer a constant as we know that LR gets phosphorylated into R_p with time. The expression of ρ_r can be obtained by assuming that the formation of LR complexes follow Michealis-Menten kinetics (rapid equilibrium approximation i.e. dissociation of $[LR]$ to $[L]+[R]$ is faster than the formation of $[R_p]$) [58] and using $[R_s] = [R]+[LR]$. This allows us to determine, ρ_r, the ratio of receptors bound to ligands to the total number of $P2Y_2$ receptors (the details are given in last section of the supplementary information)

$$\rho_r = \frac{[R_s][L]}{[R_t](K_r + [L])}$$

.

2.5 Summary of Governing Equations

Along with Equations 14 and 15, we present the expanded form of Equations 3, 6, and 13 by substituting the expressions for the fluxes mentioned in subsections 2.2 and 2.3. These equations are

$$\frac{d[R_s]}{dt} = k_r[R_t] - \left(k_r + k_p \frac{[L]}{K_r + [L]}\right)[R_s] - k_r[R_p]\,, \tag{16}$$

$$\frac{d[R_p]}{dt} = k_p \frac{[L][R_s]}{K_r + [L]} - k_e[R_p]\,, \tag{17}$$

$$\frac{d[IP_3]}{dt} = \gamma\lambda \frac{[Ca_c]}{K_1 + [Ca_c]} - k_2[IP_3]\,, \tag{18}$$

$$\frac{d[Ca_c]}{dt} = \left\{1 + \frac{[B_t]\frac{k_7}{k_6}}{\left(\frac{k_7}{k_6} + [Ca_c]\right)^2}\right\}^{-1} \left\{\left(k_3 \frac{[IP_3]^3}{K_2^3 + [IP_3]^3} \frac{K_{i,Ca_c}^3}{[Ca_c]^3 + K_{i,Ca_c}^3} + k_5\right)[Ca_s] - k_4 \frac{[Ca_c]^2}{K_3^2 + [Ca_c]^2} + k_{\text{soc}} \frac{1}{\left(1 + \frac{[Ca_s]}{K_{\text{soc}}}\right)^n} [Ca_{\text{ex}}]\left([Ca_s](0) - [Ca_s]\right) + q_{\text{in}} - k_8 \frac{[Ca_c]^2}{K_4^2 + [Ca_c]^2}\right\}, \quad (19)$$

$$\frac{d[Ca_s]}{dt} = -v_r \left\{\left(k_3 \frac{[IP]^3}{K_2^3 + [IP]^3} \frac{K_{i,Ca_c}^3}{[Ca_c]^3 + K_{i,Ca_c}^3} + k_5\right)[Ca_s] - k_4 \frac{[Ca_c]^2}{K_3^2 + [Ca_c]^2}\right\}. \quad (20)$$

Note the right hand side of the last equation contains (with opposite signs) the same first three terms in the Equation 19 due to mass conservation (these terms express the exchange between the ER and the rest of the cytoplasm).

2.6 Homeostasis concentration

The homeostatic concentration in our simulation corresponds to the initial concentration which is maintained within the EC in the absence of ligand, $[L] = 0$. The initial concentration of the cytoplasmic Ca^{2+} ($[Ca_c](0)$) and IP_3, ($[IP_3](0)$) are assumed to have typical values of 100 nM [40] and 10 nM [29], respectively. The initial ER Ca^{2+} concentration ($[Ca_s](0)$) is obtained by setting Equation 20 to zero for the given initial cytoplasmic Ca^{2+} and IP_3 concentrations. Furthermore, setting Equations 16 and 17 to zero for $[L] = 0$, we obtain the initial concentration for the unphosphorylated receptor, $[R_s](0) = [R_t]$ and the phosphorylated receptor, $[R_p](0) = 0$. The initial concentration of all these variables are listed in Table 2. The value of the constant δ (we have discussed the importance of δ in subsection 2.2) is obtained by setting Equation 18 to zero for the given initial cytoplasmic and IP_3 concentrations at $[L] = 0$, we get

$$\delta = \frac{k_2[IP_3](0)K_g}{\frac{[Ca_c](0)}{K_1 + [Ca_c](0)}\gamma - k_2[IP_3](0)}.$$

For the constant influx, q_{in}, we set Equation 19 to zero. After rearranging the obtained expression (using conditions of initial cytoplasmic and ER Ca^{2+} and IP_3), we obtain

$$q_{\text{in}} = k_8 \frac{([Ca_c](0))^2}{K_4^2 + ([Ca_c](0))^2}.$$

2.7 Parameter values

The parameter values used in this model are listed in Table 1. Most of the parameter values for the intracellular Ca^{2+} modeling are taken from [11], and a few of them are slightly adjusted in order to capture the qualitative trend of the intracellular Ca^{2+} concentration observed in experiments. The parameter values for the receptor and G-protein modeling are obtained from [29], and the value of the parameter k_p is slightly changed in order to confine the ER Ca^{2+} refilling within a timescale of 500 s (according to [9]). The importance of the parameter k_e is discussed in section 3. The k_{soc} value is also slightly adjusted to ensure that the refilling of ER occurs properly and within a timescale of 500 s. Taking the value of k_8 equal (or close) to that of k_4 guarantees a smooth decrease of the cytoplasmic Ca^{2+} concentration curve after the transient peak occurs. Moreover, we have slightly changed the values of K_2 and k_5 so that we can get the initial Ca^{2+} concentration of ER closer to the physiological concentration of 500 nM [41].

3 Results and Discussion

We have systematically solved the set of Equations 16-20 and analyzed the evolution of all the relevant variables. Inspired by several experiments [5, 42, 44, 45, 51–53], we test our model's ability to predict specific results such as calcium signal behavior due to a blockage of extracellular calcium and the response of calcium due to the removal of agonist at a particular moment after the calcium peak occurs.

Table 1 Model parameter values

Parameter	Description	Reference	Value
Receptor parameters			
k_r	Receptor recycling rate	[29]	1.75×10^{-4} s^{-1}
$[R_t]$	Total number of P2Y$_2$ receptors	[29]	2×10^4
K_r	Receptor dissociation constant	[29]	2 μM
k_p	Receptor phosphorylation rate	[29]	0.10 s^{-1}
k_e	Receptor internalized rate	[29]	6×10^{-3} s^{-1}
G-protein parameters			
k_a	G-protein activation rate	[29]	0.017 s^{-1}
k_d	G-protein deactivation rate	[29]	0.15 s^{-1}
$[G_t]$	Total number of G-protein molecules	[29]	10^5
α	Signaling gain parameter	[29]	2.781×10^{-5} s^{-1}
N_A	Avogadro's number		6.02252×10^{23} mol^{-1}
V_{EC}	Volume of EC	[13]	1.173 pl
K_1	Michelis-Menten constant		0 μM
$[(PIP_2)_t]$	Total number of PIP$_2$ molecules	[29]	5×10^4
k_2	IP$_3$ degradation rate	[11]	0.2 s^{-1}
Ca^{2+} parameters			
k_3	Ca^{2+} release rate from the ER	[11]	6.64 s^{-1}
k_4	Ca^{2+} uptake rate to the ER	[11]	5 μM s^{-1}
k_5	Ca^{2+} leak rate from the ER	(see text)	0.000545 s^{-1}
k_{soc}	Ca^{2+} influx rate via SOC	[39]	0.0086 μM^{-1} s^{-1}
n	constant	[39]	1
k_8	PMCA Ca^{2+} efflux rate	[11]	5 μM s^{-1}
K_2	Michaelis-Menten constant	[11]	0.16 μM
K_3		[11]	0.15 μM
K_4		[11]	0.32 μM
K_{i,ca_c}		[13]	1.0 μM
K_{soc}		[28]	0.1 μM
$[Ca_{\mathrm{ex}}]$	External Ca^{2+} concentration	[11]	1500 μM
v_r	Ratio of cytoplasm and ER volumes	[11]	3.5
k_6	Association rate with buffer proteins	[11]	100 μM^{-1} s^{-1}
k_7	Dissociation rate with buffer proteins	[11]	300 s^{-1}
$[B_t]$	Total buffer protein concentration	[11]	120 μM

3.1 General discussion of the outcome of the model

In this section we are going first to describe the main results implied by our model, while in the next section we will directly confront directly some of our predictions with existing experiments.

3.1.1 Receptor desensitization affects intracellular homeostasis

An interesting fact is that (see Figure 4) the model shows that when an EC is stimulated with a constant ATP concentration, i.e., $[L] = 300$ nM for a long period of time, the intracellular concentration of IP$_3$ (Figure 4(c)), intracellular cytoplasmic Ca^{2+} (Figure 4(d)), and ER Ca^{2+} (Figure 4(e)) return naturally back to their initial concentration (homeostasis). This behavior is related to the exponential decay of unphosphorylated receptor concentration as shown in Figure 4(a), which in turn causes a decrease in IP$_3$ generation after a transient peak at 15 s as shown in Figure 4(c). However, the transient peak time is dose-dependent; for example, the higher the ATP concentration, the faster are the EC

Table 2 Model initial conditions

Parameters	Description	Value
$[R_s]\,(0)$	Unphosphorylated receptors	$[R_t]$
$[R_p]\,(0)$	Phosphorylated receptors	0
$[IP_3]\,(0)$	IP_3 concentration	0.01 μM
$[Ca_c]\,(0)$	Cytoplasmic Ca^{2+} concentration	0.1 μM
$[Ca_s]\,(0)$	ER Ca^{2+} concentration	711.0 μM

response and IP_3 transient peak. Figure 4(d)) shows that the cytoplasmic Ca^{2+} and IP_3 peak occur approximately at the same time. This is a direct consequence of the fact that a maximum of IP_3 leads to a maximal release from the internal store. Another fact is that due to a prolonged presence of ligand, the concentration of unphosphorylated receptor continuously decreases to approach a minimal value, leading to desensitization of receptors, so that IP_3 concentration is able to return to its homeostatic concentration. This also triggers a decrease in Ca^{2+} release from the ER, whereas Ca^{2+} uptake from the cytoplasm (through the SERCA, as shown in Figure 4(e)) continues to operate allowing for a refilling of the internal store (ER). Moreover, as long as the ATP remains in the plasma, the unphosphorylated receptor concentration remains at its minimal concentration. Note that a higher unphosphorylated receptor concentration can be obtained by increasing the rate constants k_e and k_r. These constants are responsible for the conversion of phosphorylated receptors to the unbound receptors by following two steps, i.e., R_p to R_I and R_I to R. Additionally, the phosphorylated receptors reach a transient peak (as shown in Figure 4(b)) due to the availability of a minimal number of unphosphorylated receptors to bind with the external ATP in order to form phosphorylated receptors. From Figure 4(b), it is also evident that the phosphorylated receptor concentration decreases slowly due to the recycling of phosphorylated receptors to unbound receptors by undergoing an intermediate receptor state, R_I.

It is worthwhile to emphasize the main difference between the present model and previous ones [9–15]. One of the main criticisms is that previous models of EC Ca^{2+} do not recover the evolution with time towards intracellular homeostasis for any of the quantities at play namely, $[i(t)]$, $[Ca_c(t)]$, and $[Ca_s(t)]$), as shown in Figure S1 (supplementary information). Figure S1 (supplementary information) demonstrates that the intracellular concentrations remain significantly above the initial concentration when the EC is stimulated with a constant ATP, $[L] = 300$ nM. The present model is able to recover the homeostatic conditions provided the receptor desensitization is taken into account.

3.1.2 Faster intracellular homeostasis in absence of ATP

Most of the experiments [5, 42] have been performed by stimulating ECs for a fixed period of time with a constant ligand concentration followed by washing the stimulus away in order to investigate the trailing cytoplasmic Ca^{2+} concentration in the absence of the ligand. The trailing cytoplasmic Ca^{2+} concentration refers to the concentration after the transient peak. It has been found [42] that the cytoplasmic Ca^{2+} concentration immediately returns to its initial concentration when ATP is removed after stimulating the EC for any period of time. However, no experimental data are available for the ER Ca^{2+} and IP_3 concentrations due to the experimental difficulties associated with obtaining these values. We have simulated this experimental scenario (the return of cytoplasmic Ca^{2+} to its initial concentration) by setting the ATP concentration to zero (i.e., $[L] = 0$) after stimulating an EC for 150 s. Figure 4(a) (black dotted line) shows that the unphosphorylated receptor concentration increases due to the conversion of phosphorylated to unbound receptors. This increase is inevitable because of the absence of ATP and hence its inability to phosphorylate the unbound receptors. As a consequence, the IP_3 concentration immediately returns to its initial level at the time when ATP is removed from the plasma, as shown in Figure 4(c). Furthermore, cytoplasmic Ca^{2+} (as shown in Figure

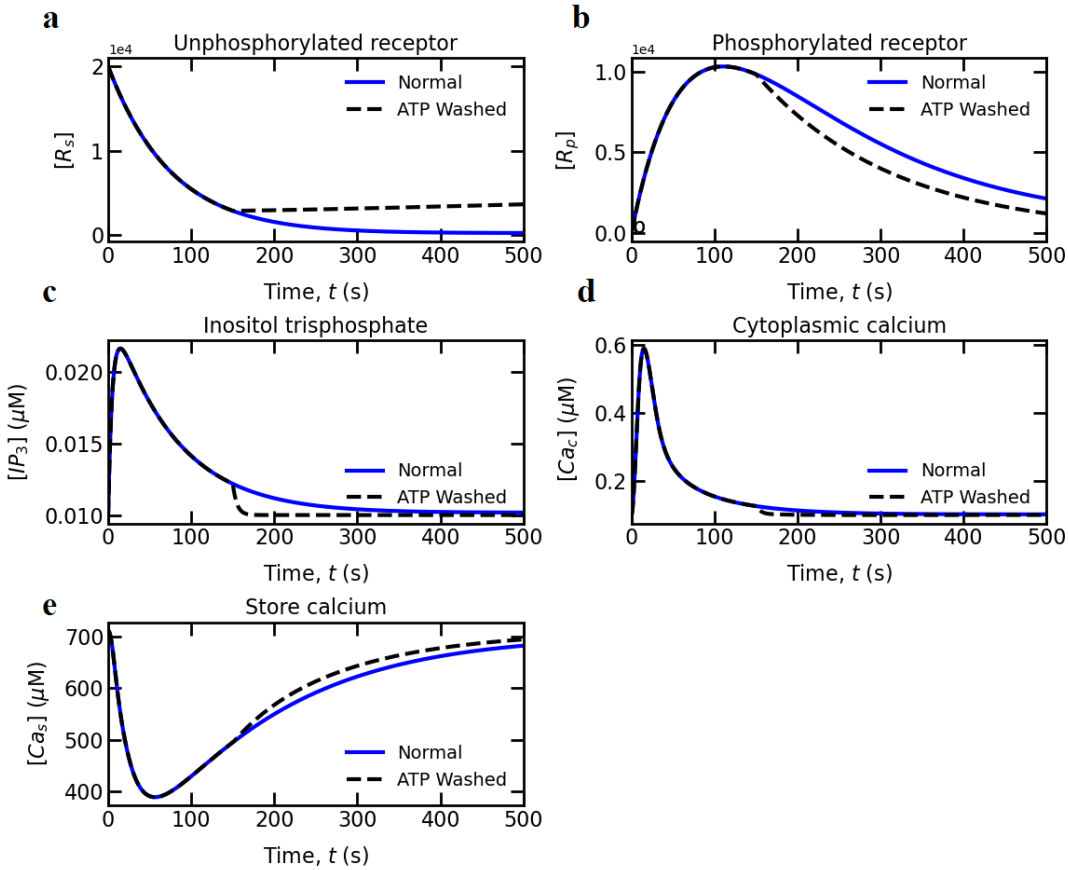

Fig. 4 Variation of concentrations with time for a single EC stimulated by a constant ATP, $[L] = 300$ nM: (a) unphosphorylated receptor concentration; (b) phosphorylated receptor concentration; (c) inositol trisphosphate concentration; (d) cytoplasmic Ca^{2+} concentration; (e) store Ca^{2+} concentration. **Normal** refers to the case when an EC is stimulated for 500 s, and **ATP Washed** refers to the case when an EC is stimulated for 150 s.

4(d)) reverts to its initial concentration due to the pumping of cytoplasmic Ca^{2+} to the ER and the extracellular space. Additionally, Figure 4(e) shows that the ER is completely refilled to its initial concentration. This is due only to Ca^{2+} uptake from the cytoplasm rather than to Ca^{2+} release from the ER to the cytoplasm in the absence of IP_3. Thus, Figure 4 clearly reveals that intracellular homeostasis is achieved faster in the absence of ATP than in the case of maintaining a constant ATP for a prolonged period, which means that EC intracellular homeostasis basically depends upon the ATP stimulation time.

3.1.3 Extracellular Ca^{2+} is responsible for ER refilling

Some Ca^{2+} dynamics models are able to explain the oscillations in intracellular Ca^{2+} concentrations without considering Ca^{2+} fluxes across the PM [4, 8]. However, in most experiments [4, 5] on ECs, a single transient peak followed by a plateau has been observed. This behavior results from the balance between Ca^{2+} fluxes across the ER membrane and the PM. In order to experimentally elucidate the role of extracellular Ca^{2+} in maintaining the cytoplasmic and ER Ca^{2+} homeostatic concentrations, as well as to understand the pathways [43–45] and the regulation of downstream molecules [46], the Ca^{2+} chelating agent EGTA is commonly added to the extracellular solution

where it binds with the free extracellular Ca^{2+}. The binding of Ca^{2+} to EGTA blocks the influx of Ca^{2+} from the extracellular environment into the cytoplasm. To understand the effect of EGTA in the simulations, we have set q_{in} and q_{soc} to zero. This has two consequences (see in Figure 5): (i) the trailing (or steady) cytoplasmic concentration is lower than its initial concentration, and (ii) the ER Ca^{2+} continues to be depleted, without any tendency of refilling towards its homeostatic concentration. Both facts are in agreement with experiments [47] and [48]. In conclusion of this section, the inhibition of calcium entry from the extracellular space leads to undershooting of intracellular calcium, and the lack of refilling of ER Ca^{2+}. In both cases, the relevant pathway is associated with the SOC; as seen in Equation **??**, the corresponding flux results from the deviation from homeostatic ER concentration, and its inhibition precludes the ER from getting back to homeostasis. We found that among the two influxes across the cytoplasmic membrane (q_{min} and q_{soc}), the SOC is dominant, in agreement with experimental findings [45, 48].

3.1.4 Variation of Ca^{2+} transient peak in ECs due to the receptor affinity

In experiments, it has been reported that a given ligand concentration can yield different amplitudes of cytoplasmic Ca^{2+} peaks for individual cells originating from the same cell line [49]. Furthermore, when considering the same origin of ECs subjected to different agonists at the same concentration, it has been observed that the Ca^{2+} peak amplitude depends on the type of ligand [5, 50]. The first observation may be explained as being due to intercellular differences in the receptor concentration, the size of the cell, PLC activity or ER Ca^{2+} capacity [49], whereas the second observation may attributable to variations in ligand affinity to their respective membrane receptors. This second observation (different agonists with the same EC) lends itself to a simpler interpretation as compared to the first one. Different agonists are expected to have different receptor affinity. We have thus explored this scenario by varying the dissociation constant, K_r, in the range of 0.8-12.5 μM for a fixed 300 nM ligand concentration. Figure 6(b) displays the effect of affinity on the cytoplasmic Ca^{2+} peak. Note that increasing the receptor dissociation constant, K_r, means a weaker interaction between the $P2Y_2$ receptor and the ligand. This naturally leads to a decrease in cytoplasmic Ca^{2+} peak since this implies a slower decay of unphosphorylated receptors, resulting in fewer IP_3 molecule formation as shown in Figure 6(a). The first observation (i.e., different cells of the same cell line produce different amplitudes) can be explained by randomly selecting parameter values from the Gaussian distribution around the mean parameter values [49].

3.1.5 Saturation of transient peak with increasing ATP concentration

Figure 7 shows that the cytoplasmic Ca^{2+} peak concentration gets saturated with increasing of ATP concentration. The dependence of the cytoplasmic Ca^{2+} peak on ATP concentration is sigmoidal, which is commonly encountered in many biological processes. This is due to the fact that the decay of the unphosphorylated receptors is fast. As a result, IP_3 formation gets saturated with the fast decay of unphosphorylated receptors. Due to the saturation of IP_3 formation, a fixed quantity of Ca^{2+} is released from the ER that leads to saturation of the cytoplasmic Ca^{2+} peak.

3.1.6 Elevated cytoplasmic Ca^{2+} depends on receptor recycling rate

Many experimental studies have reported that the steady state cytoplasmic Ca^{2+} concentration (the plateau after the peak) can sometimes be more than double that of the initial concentration [44, 51–53]. This means that the cell may not return to its homeostatic condition, as one would expect *in vivo*. We have seen before that our model can account for homeostatic recovery, provided the phosphorylated receptor recycling rate k_r is sufficiently small enough (see Figure 4). However, if the recycling rate is varied, our model can still capture the fact that the final Ca^{2+} concentration is higher than the homeostatic one. Figure 8(a) shows that an increase in k_r, results in a higher steady unphosphorylated receptor concentration. This means that the phosphorylated

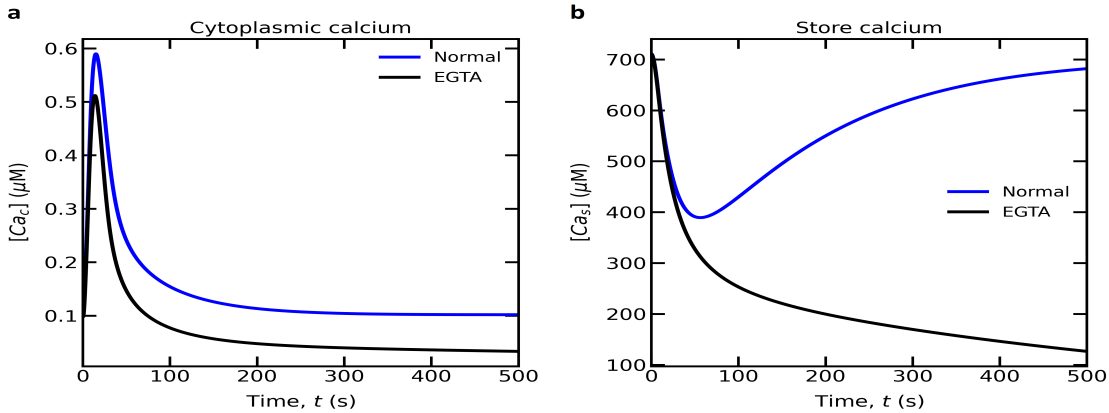

Fig. 5 Comparison of theoretical model variable results for a single EC stimulated by a constant ATP, $[L] = 300$ nM under physiological conditions (**Normal**) and no external Ca^{2+} (**EGTA**): (a) cytoplasmic Ca^{2+} concentration; (b) store Ca^{2+} concentration.

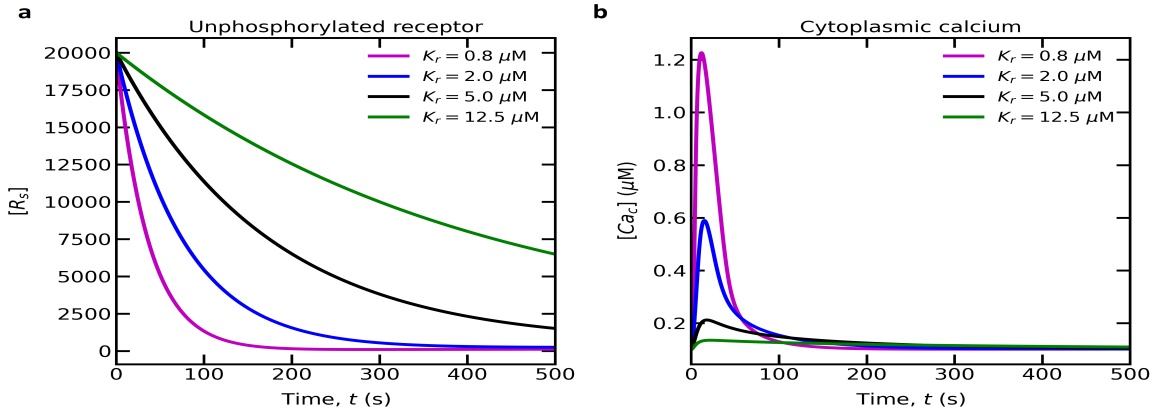

Fig. 6 Theoretical model variable results for a single EC stimulated with $[L] = 300$ nM and by varying the $P2Y_2$ receptor dissociation constant, K_r: (a) unphosphorylated receptor concentration; (b) cytoplasmic Ca^{2+} concentration.

receptors are rapidly recycled into unphosphorylated receptors in the presence of sufficiently high ATP concentration. However, the initial decaying of unphosphorylated receptors remains unchanged with changing k_r. The cytoplasmic Ca^{2+} concentration change (as shown in Figure 8(b)) is due to the elevated unphosphorylated concentration. As long as the unphosphorylated receptor concentration remains elevated, IP_3 molecules are continuously activated, triggering further release of Ca^{2+} from the ER. However, no change in the cytoplasmic Ca^{2+} transient peak is observed upon variation of k_r. In conclusion, it is tempting to speculate that the non recovery of homeostasis may be associated with an *in vitro* alteration of the recycling rate.

3.2 Direct model confrontation with experimental data

Here we confront our model with several experimental results. In order to make a comparison with the proposed model results, we have dimensionalized the cytoplasmic Ca^{2+} concentrations with their corresponding maximum cytoplasmic Ca^{2+} concentrations.

3.2.1 Calcium homeostasis recovery

In an experimental study by Carter et al. [5], the response (cytoplasmic Ca^{2+} concentration) of a human umbilical-vein EC (HUVEC) is analyzed by stimulating ECs with 100 μM concentrations of ATP. At the beginning of the stimulation, a rapid rise in the cytoplasmic Ca^{2+} concentration

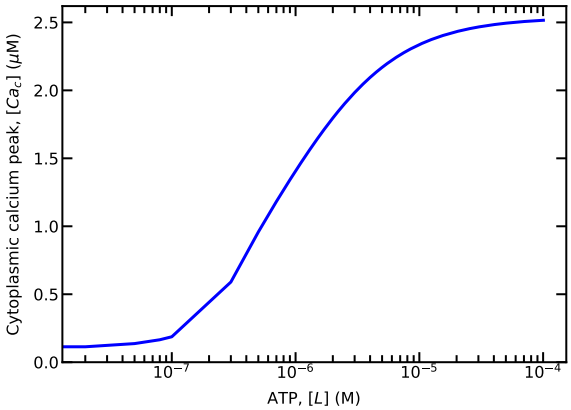

Fig. 7 Variation of peak cytoplasmic Ca^{2+} concentration with ATP, $[L]$ concentration

from its basal concentration is observed. This is due to the release of IP_3 dependent Ca^{2+} from the ER. The cytoplasmic Ca^{2+} concentration reaches a peak at $\sim$ 6 s and subsequently, it returns to its basal concentration. Their results are reported in Figure 9(a) (symbols). We have confronted our model to this observation by taking the same ATP concentration as in the experiments. Our results are shown in Figure 9(a) (solid line). Overall the model reproduces reasonably well the recovery towards homeostasis and the duration of the peak. It must be noted, however, that if the non-dimensionlized result of the cytoplasmic Ca^{2+} concentration of our model agrees with the non-dimensionalized experimental result, our model overestimates the amplitude of maximal calcium peak (see inset in Figure 9(a)), when the physical value of cytoplasmic Ca^{2+} concentration is compared (instead of dimensionalized one). Certainly more systematic adaptation of model parameters is required to have a better agreement of the model and experimental results. We have tried to find the proper parameters in order to have better agreement of the physical cytoplasmic Ca^{2+} concentration of our result with the experimental result. We have attempted to vary the values of kinetic constant k_2 (the IP_3 degradation rate constant; Equation 18) from 0.2 to 0.62 s^{-1}. These value are within the range of values reported in the experiments, namely $k_2 \simeq$ 0.001-2 s^{-1} [49]. Taking for k_2 =0.62 s^{-1} provides a much better agreement (Fig.9(b)).

3.2.2 Homologous receptor desensitization

A central question concerns the ECs response to a second ATP stimulation after a first stimulation has been applied for a certain time and then washed out. To answer this question Carter et al. [5] have performed an experimental study to answer this question. For that purpose they applied ATP to ECs for a certain time, then removed it for some time, before stimulating again with ATP. Figure 9(c) shows that stimulating again ECs by ATP leads to no subsequent cytoplasmic Ca^{2+} response. In fact they have shown that a second calcium response due to second ATP stimulation, is seen only if the second ATP stimulation takes place after some time (from 5 to 20 min). As anticipated when building our model, this observation is a hint to the existence of some desensitization of receptors by ATP. The result from our model also reveal the absence of calcium response after a second stimulation. This is to be contrasted with other models [26, 27] which predict an immediate response of the cell following the application of agonist (Figure S4, supplementary information). Note, however, that a second response of ECs requires a maximum time of 20 min to respond a second ATP stimulation, whereas our model predicts about more than 2 hr (see inset Figure 9(c)). Here again, we did not enforce our parameters to provide a better agreement, but have selected most of parameters from several experimental estimates. Still, we believe that further improvement will be possible in the future, by looking for best fits, as we did above for k_2. We hope to dig further into this question in a future work.

3.2.3 Role of the extracellular calcium on homeostasis

In another experimental validation of the proposed model, we used the experimental result of Yamamoto et al. [59] in which they measured the cytoplasmic Ca^{2+} concentration in the presence of exogenous EGTA (ethylene glycol-bis-N,N,N',N'-tetraacetic acid). EGTA binds to free extracellular calcium, preventing then extracellular calcium to enter the cytoplasm. They found that the final (Figure 9(d)) cytoplasmic calcium concentration is lower than the initial one (i.e. lack of homeostasis).

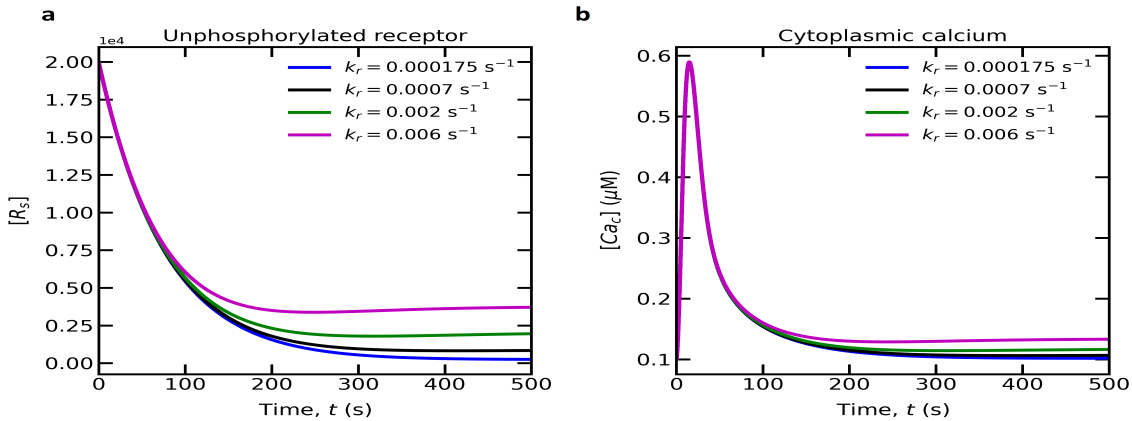

Fig. 8 Theoretical model variable results for a single EC stimulated by a constant ATP, $[L] = 300$ nM as a function of the receptor recycling rate constant, k_r: (a) unphosphorylated receptor concentration; (b) cytoplasmic Ca^{2+} concentration.

This indicates that extracellular calcium is essential for recovery of initial cytoplasmic calcium concentration. We have simulated this experiment by setting q_{soc} and q_{in} (entering Equation 19) to zero (further discussions about the effects of EGTA on the cytoplasmic and store Ca^{2+}, has been given in subsection 3.1.3). The predicted result regarding the decrease in the dimensionless cytoplasmic Ca^{2+}, after the peak of cytoplasmic Ca^{2+}, has a good agreement with the experimental result (Figure 9(d)).

Finally some remarks are in order. Due to the limited availability of experimental data for the ER Ca^{2+} and IP_3 concentrations, we have focused on the validation of the experimental cytoplasmic Ca^{2+} since measurement of cytoplasmic Ca^{2+} concentration with the help of fluorescence is relatively easier than the ER Ca^{2+}. Owing to difficulties in loading the Ca^{2+}-sensing fluorescent dyes in the ER [60], it is rarely measured in experiments. However, several new technologies [62, 63] have been developed to measure the ER Ca^{2+} concentrations but it is still a matter of debate regarding the accuracy of the measured data. Similarly there are certain difficulties associated with the quantitative measurement of IP_3 molecules and tracking of PIP_2 molecules from where IP_3 molecules are formed [61]. Therefore most reported data focus on cytoplasmic Ca^{2+} concentrations. However, the complete validation of Ca^{2+} dynamics model with all the measured intracellular Ca^{2+} dynamics variables, such as IP_3, Ca_c, and Ca_s, would be an interesting topic for future research.

4 Conclusion

In this work, we have developed a homeostatic Ca^{2+} dynamics model in which the intracellular EC homeostasis depends on receptor dynamics. We have shown that the model is able to capture various experimental observations including the effect of stimulating ECs with ATP for a fixed time before washing the stimulus out, the extracellular Ca^{2+}-dependent ER Ca^{2+} refilling, the reason for varying Ca^{2+} transients in different experiments on even in the same EC, the saturation of cytoplasmic Ca^{2+} with increasing ATP concentration, and the cause of elevated cytoplasmic Ca^{2+} concentration levels.

The current Ca^{2+} model is primarily focused on how the EC is able to manage intracellular homeostatic concentrations in the presence of ATP. However, in the experiment of Carter et al. [5], some of the ECs exhibit oscillation of cytoplasmic Ca^{2+} concentration. It would be interesting to enrich our model in order to account for oscillations. Several models in the past have successfully accounted for Ca^{2+} oscillation in the presence of agonists as discussed at the beginning of the introduction. Inspired by several models [19, 21–26], leading to the oscillation, we believe that incorporating additional feedback pathways (either positive or negative or both) into the model is necessary. We have in mind certain feedback pathways which would control the dynamics of receptors. For instance, the response of the present model due to ATP is controlled by the competition between the timescales of phosphorylation

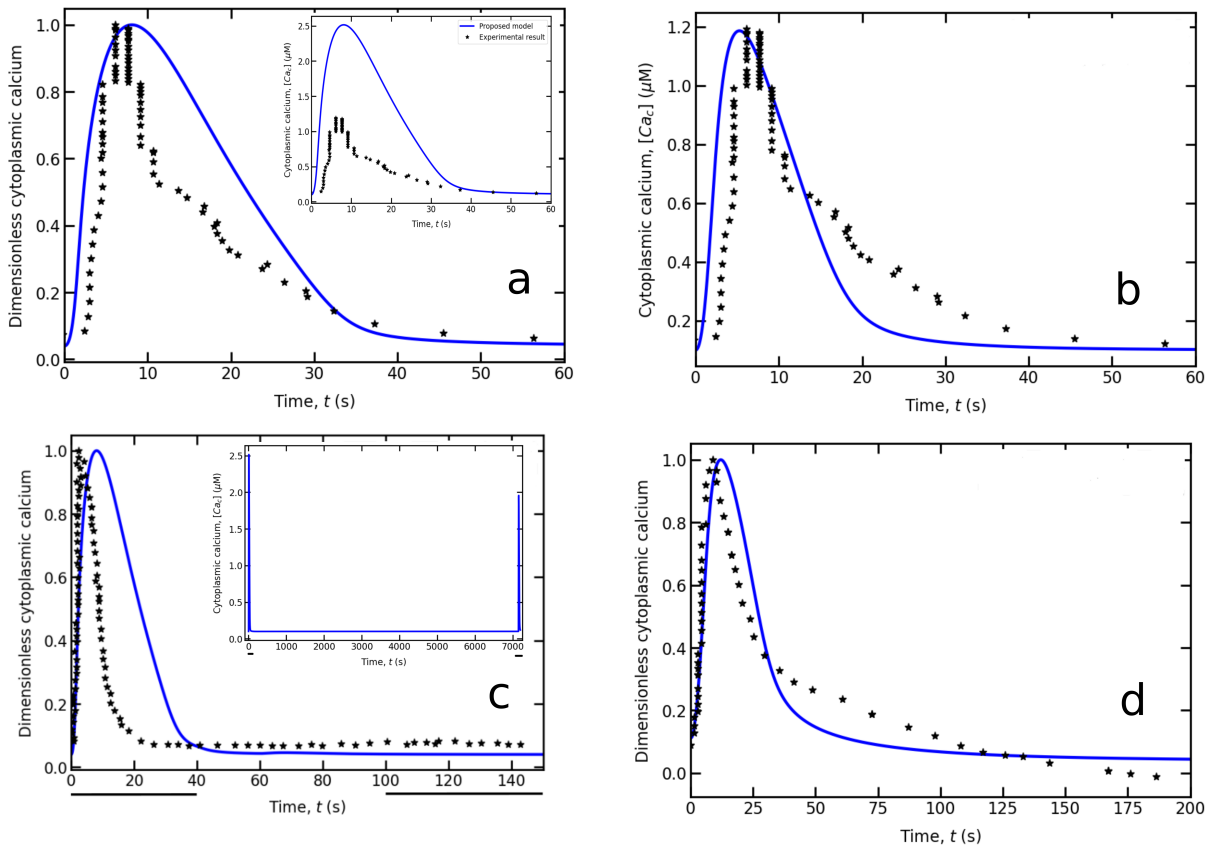

Fig. 9 Experimental validations of the proposed Ca^{2+} dynamics model: (a) the comparison of the dimensionless cytoplasmic Ca^{2+} concentration obtained from the proposed model with the experimental result is done in the presence of 100 μM of ATP concentrations for 60 s (Experimental result: Figure 1(a) [5]). Inset represents the comparison of physical cytoplasmic Ca^{2+} concentration of the proposed model with the experimental result. (b) A better agreement result (extension of Figure 9(a)) between the physical cytoplasmic Ca^{2+} concentration of the proposed model and the experimental result is acquired by setting the parameter k_2 to 0.62 s^{-1} (Equation 18); (c) the dimensionless cytoplasmic Ca^{2+} concentration is obtained when the EC is stimulated with 100 μM concentrations of ATP for 40 s and followed by washing out ATP from the solution and it is then applied after 60 s for 40 s (Experimental result: Figure 2 [5]). Inset shows the time taken by the EC to respond the second dose of 100 μM concentrations of ATP (model prediction). The black bold line (below x-axis) represents the time at which ATP is injected into the solution; (d) the trailing dimensionless cytoplasmic Ca^{2+} concentration is obtained when the EC is stimulated with 500 nM of ATP concentrations in the presence of chelator, EGTA (ethylene glycol-bis-N,N,N',N'-tetraacetic acid) in the extracellular space (Experimental result: Figure 1(c) [59]).

of the free receptors and formation of the free receptors from the phosphorylated receptors. In order to favor oscillations, these timescales must be tuned with the feedback pathways from downstream reactions as well as with the dynamics of intracellular variables. For that purpose, a well-designed experimental protocol would be needed to gain insight into the receptor controlling feedback pathways. This would lead to an interesting future research perspective.

Finally, in a recent work, Zhang et al. [54] have proposed a phenomenological ATP release model when RBCs are subjected to flow. The concentration of ATP in fluid, bloodstream, depends on the several factors [55] such as geometry of vascular network, flow condition, hematocrit concentration, and enzymatic reaction of enzymes present on the EC surface. These ATP molecules finally lead to activation of calcium signaling in ECs. In order to understand the effects of RBC dynamics and vascular diseases such as atherosclerosis, aneurysm, and stroke on EC response, it is indispensable to study two things together. In addition, a through study, the coupling between the RBC's ATP release and EC Ca^{2+} signaling, is

needed intending to understand the origin of EC related diseases.

In future work, we would like to study the blood flow simulation by explicitly taking into account RBCs and their ATP release as well as reaction with ECs triggering calcium for simple and complex vascular networks.

Supplementary Information

An online supplement to this article can be found by visiting Online at https://www.springer.com/journal/10237/.

Acknowledgments

We acknowledge the financial support from CNES (Centre National d'Etudes Spatiales) and for having access to data, and the French-German University Programme Living Fluids (Grant CFDA-Q1-14). The simulations were performed on the Cactus cluster of the CIMENT infrastructure, which is supported by the Rhône-Alpes region (Grant No. CPER07 13 CIRA).

Author Contributions

Ananta Kumar Nayak developed the calcium model and analyzed it. Zhe Gou, Sovan Lal Das, Abdul I. Barakat and Chaouqi Misbah participated to model development and interpretation. Chaouqi Misbah has designed the research topic and planes. All the authors have contributed to the paper writing and interpretations.

Declaration of Interests

The authors declare that they have no conflict of interest.

References

[1] Berridge, M. J., M. D. Bootman, and H. L. Roderick, 2003. Calcium signalling: dynamics, homeostasis and remodelling. *Nature reviews Molecular cell biology* 4:517–529.

[2] Tran, Q.-K., K. Ohashi, and H. Watanabe, 2000. Calcium signalling in endothelial cells. *Cardiovascular research* 48:13–22.

[3] Shen, J., F. W. Luscinskas, A. Connolly, C. F. Dewey Jr, and M. Gimbrone Jr, 1992. Fluid shear stress modulates cytosolic free calcium in vascular endothelial cells. *American Journal of Physiology-Cell Physiology* 262:C384–C390.

[4] Sage, S. O., D. J. Adams, and C. Van Breemen, 1989. Synchronized oscillations in cytoplasmic free calcium concentration in confluent bradykinin-stimulated bovine pulmonary artery endothelial cell monolayers. *Journal of Biological Chemistry* 264:6–9.

[5] Carter, T., J. Newton, R. Jacob, and J. Pearson, 1990. Homologous desensitization of ATP-mediated elevations in cytoplasmic calcium and prostacyclin release in human endothelial cells does not involve protein kinase C. *Biochemical journal* 272:217–221.

[6] Xu, S., X. Li, K. B. LaPenna, S. D. Yokota, S. Huke, and P. He, 2017. New insights into shear stress-induced endothelial signalling and barrier function: cell-free fluid versus blood flow. *Cardiovascular research* 113:508–518.

[7] Davignon, J., and P. Ganz, 2004. Role of endothelial dysfunction in atherosclerosis. *Circulation* 109:III–27.

[8] Meyer, T., and L. Stryer, 1988. Molecular model for receptor-stimulated calcium spiking. *Proceedings of the National Academy of Sciences* 85:5051–5055.

[9] Wiesner, T. F., B. C. Berk, and R. M. Nerem, 1996. A mathematical model of cytosolic calcium dynamics in human umbilical vein endothelial cells. *American Journal of Physiology-Cell Physiology* 270:C1556–C1569.

[10] Wiesner, T. F., B. C. Berk, and R. M. Nerem, 1997. A mathematical model of the cytosolic-free calcium response in endothelial cells to fluid shear stress. *Proceedings of the National Academy of Sciences* 94:3726–3731.

[11] Plank, M. J., D. J. Wall, and T. David, 2006. Atherosclerosis and calcium signalling in endothelial cells. *Progress in biophysics and molecular biology* 91:287–313.

[12] Plank, M., D. Wall, and T. David, 2007. The role of endothelial calcium and nitric oxide in the localisation of atherosclerosis. *Mathematical biosciences* 207:26–39.

[13] Silva, H. S., A. Kapela, and N. M. Tsoukias, 2007. A mathematical model of plasma membrane electrophysiology and calcium dynamics in vascular endothelial cells. *American Journal of Physiology-Cell Physiology* 293:C277–C293.

[14] Comerford, A., M. Plank, and T. David, 2008. Endothelial nitric oxide synthase and calcium production in arterial geometries: an integrated fluid mechanics/cell model. *Journal of biomechanical engineering* 130.

[15] Li, L.-F., C. Xiang, and K.-R. Qin, 2015. Modeling of $TRPV_4$-C_1-mediated calcium signaling in vascular endothelial cells induced by fluid shear stress and ATP. *Biomechanics and modeling in mechanobiology* 14:979–993.

[16] Dupont, G., and A. Goldbeter, 1993. One-pool model for Ca^{2+} oscillations involving Ca^{2+} and inositol 1, 4, 5-trisphosphate as co-agonists for Ca^{2+} release. *Cell calcium* 14:311–322.

[17] Atri, A., J. Amundson, D. Clapham, and J. Sneyd, 1993. A single-pool model for intracellular calcium oscillations and waves in the Xenopus laevis oocyte. *Biophysical Journal* 65:1727–1739.

[18] Shen, P., and R. Larter, 1995. Chaos in intracellular Ca^{2+} oscillations in a new model for non-excitable cells. *Cell calcium* 17:225–232.

[19] Dupont, G., and C. Erneux, 1997. Simulations of the effects of inositol 1, 4, 5-trisphosphate 3-kinase and 5-phosphatase activities on Ca^{2+} oscillations. *Cell calcium* 22:321–331.

[20] Borghans, J. M., G. Dupont, and A. Goldbeter, 1997. Complex intracellular calcium oscillations A theoretical exploration of possible mechanisms. *Biophysical chemistry* 66:25–41.

[21] Marhl, M., T. Haberichter, M. Brumen, and R. Heinrich, 2000. Complex calcium oscillations and the role of mitochondria and cytosolic proteins. *Biosystems* 57:75–86.

[22] Kummer, U., L. F. Olsen, C. J. Dixon, A. K. Green, E. Bornberg-Bauer, and G. Baier, 2000. Switching from simple to complex oscillations in calcium signaling. *Biophysical journal* 79:1188–1195.

[23] Schuster, S., M. Marhl, and T. Höfer, 2002. Modelling of simple and complex calcium oscillations: From single-cell responses to intercellular signalling. *European Journal of Biochemistry* 269:1333–1355.

[24] Politi, A., L. D. Gaspers, A. P. Thomas, and T. Höfer, 2006. Models of IP_3 and Ca^{2+} oscillations: frequency encoding and identification of underlying feedbacks. *Biophysical journal* 90:3120–3133.

[25] Dupont, G., E. F. L. Lokenye, and R. J. Challiss, 2011. A model for Ca^{2+} oscillations stimulated by the type 5 metabotropic glutamate receptor: an unusual mechanism based on repetitive, reversible phosphorylation of the receptor. *Biochimie* 93:2132–2138.

[26] Cuthbertson, K., and T. Chay, 1991. Modelling receptor-controlled intracellular calcium oscillators. *Cell calcium* 12:97–109.

[27] Wang, J., X. Huang, and W. Huang, 2007. A quantitative kinetic model for ATP-induced intracellular Ca^{2+} oscillations. *Journal of theoretical biology* 245:510–519.

[28] Kapela, A., A. Bezerianos, and N. M. Tsoukias, 2008. A mathematical model of Ca^{2+} dynamics in rat mesenteric smooth muscle cell: agonist and NO stimulation. *Journal of theoretical biology* 253:238–260.

[29] Lemon, G., W. Gibson, and M. Bennett, 2003. Metabotropic receptor activation, desensitization and sequestration-I: modelling calcium and inositol 1, 4, 5-trisphosphate dynamics following receptor activation. *Journal of Theoretical Biology* 223:93–111.

[30] Putney Jr, J. W., 1986. A model for receptor-regulated calcium entry. *Cell calcium* 7:1–12.

[31] Putney, J. W., L. M. Broad, F.-J. Braun, J.-P. Lievremont, and G. S. J. Bird, 2001. Mechanisms of capacitative calcium entry. *Journal of cell science* 114:2223–2229.

[32] Garrad, R. C., M. A. Otero, L. Erb, P. M. Theiss, L. L. Clarke, F. A. Gonzalez, J. T. Turner, and G. A. Weisman, 1998. Structural basis of agonist-induced desensitization and sequestration of the P2Y2 nucleotide receptor: consequences of truncation of the C terminus. *Journal of Biological Chemistry* 273:29437–29444.

[33] Felix, J. A., M. L. Woodruff, and E. R. Dirksen, 1996. Stretch increases inositol 1, 4, 5-trisphosphate concentration in airway epithelial cells. *American journal of respiratory cell and molecular biology* 14:296–301.

[34] Nollert, M., S. Eskin, and L. McIntire, 1990. Shear stress increases inositol trisphosphate levels in human endothelial cells. *Biochemical and biophysical research communications* 170:281–287.

[35] Bennett, M., L. Farnell, and W. Gibson, 2005. A quantitative model of purinergic junctional transmission of calcium waves in astrocyte networks. *Biophysical journal* 89:2235–2250.

[36] Wagner, J., and J. Keizer, 1994. Effects of rapid buffers on Ca^{2+} diffusion and Ca^{2+} oscillations. *Biophysical journal* 67:447–456.

[37] Dupont, G., M. Falcke, V. Kirk, and J. Sneyd, 2016. Models of calcium signalling, volume 43. Springer.

[38] Thillaiappan, N. B., P. Chakraborty, G. Hasan, and C. W. Taylor, 2019. IP_3 receptors and Ca^{2+} entry. *Biochimica Et Biophysica Acta (BBA)-Molecular Cell Research* 1866:1092–1100.

[39] Su, J., F. Xu, X. Lu, and T. Lu, 2011. Fluid flow induced calcium response in osteoblasts: mathematical modeling. *Journal of biomechanics* 44:2040–2046.

[40] Billaud, M., A. W. Lohman, S. R. Johnstone, L. A. Biwer, S. Mutchler, and B. E. Isakson, 2014. Regulation of cellular communication by signaling microdomains in the blood vessel wall. *Pharmacological reviews* 66:513–569.

[41] Pecze, L., W. Blum, and B. Schwaller, 2015. Routes of Ca^{2+} shuttling during Ca^{2+} oscillations: focus on the role of mitochondrial Ca^{2+} handling and cytosolic Ca^{2+} buffers. *Journal of Biological Chemistry* 290:28214–28230.

[42] Mo, M., S. G. Eskin, and W. P. Schilling, 1991. Flow-induced changes in Ca^{2+} signaling of vascular endothelial cells: effect of shear stress and ATP. *American Journal of Physiology-Heart and Circulatory Physiology* 260:H1698–H1707.

[43] Lückhoff, A., and R. Busse, 1986. Increased free calcium in endothelial cells under stimulation with adenine nucleotides. *Journal of cellular physiology* 126:414–420.

[44] Yang, S.-W., W. K. Lee, E.-J. Lee, K.-A. Kim, Y. Lim, K.-H. Lee, H. K. Rha, and T.-W. Hahn, 2001. Effect of bradykinin on cultured bovine corneal endothelial cells. *Ophthalmologica* 215:303–308.

[45] Malli, R., M. Frieden, M. Trenker, and W. F. Graier, 2005. The role of mitochondria for Ca^{2+} refilling of the endoplasmic reticulum. *Journal of Biological Chemistry* 280:12114–12122.

[46] Carter, T., and J. Pearson, 1992. Regulation of prostacyclin synthesis in endothelial cells. *Physiology* 7:64–69.

[47] Yamarnoto, N., H. Watanabe, H. Kakizawa, M. Hirano, A. Kobayashi, and R. Ohno,

1995. A study on thapsigargin-induced calcium ion and cation influx pathways in vascular endothelial cells. *Biochimica et Biophysica Acta (BBA)-Molecular Cell Research* 1266:157–162.

[48] Malli, R., M. Frieden, M. Hunkova, M. Trenker, and W. Graier, 2007. Ca^{2+} refilling of the endoplasmic reticulum is largely preserved albeit reduced Ca^{2+} entry in endothelial cells. *Cell calcium* 41:63–76.

[49] Mahama, P. A., and J. J. Linderman, 1994. Calcium signaling in individual BC3H1 cells: Speed of calcium mobilization and heterogeneity. *Biotechnology progress* 10:45–54.

[50] van IJzendoorn, S., R. van Gool, C. Reutelingsperger, and J. Heemskerk, 1996. Unstimulated platelets evoke calcium responses in human umbilical vein endothelial cells. *Biochim Biophys Acta* 1311:64–70.

[51] Colden-Stanfield, M., W. P. Schilling, A. K. Ritchie, S. G. Eskin, L. T. Navarro, and D. L. Kunze, 1987. Bradykinin-induced increases in cytosolic calcium and ionic currents in cultured bovine aortic endothelial cells. *Circulation research* 61:632–640.

[52] Jacob, R., J. E. Merritt, T. J. Hallam, and T. J. Rink, 1988. Repetitive spikes in cytoplasmic calcium evoked by histamine in human endothelial cells. *Nature* 335:40–45.

[53] Zhu, L., and P. He, 2005. Platelet-activating factor increases endothelial $[Ca^{2+}]_i$ and NO production in individually perfused intact microvessels. *American Journal of Physiology-Heart and Circulatory Physiology* 288:H2869–H2877.

[54] Zhang, H., Z. Shen, B. Hogan, A. I. Barakat, and C. Misbah, 2018. ATP release by red blood cells under flow: model and simulations. *Biophysical journal* 115:2218–2229.

[55] Gou, Z., H. Zhang, M. Abbasi, and C. Misbah, 2021. Red blood cells under flow show maximal ATP release for specific hematocrit. *Biophysical Journal* 120:4819–4831.

[56] Mirianas Chachisvilis, Yan-Liang Zhang, and John A Frangos, 2006. G protein-coupled receptors sense fluid shear stress in endothelial cells. *Proceedings of the National Academy of Sciences*, 103:15463–15468.

[57] Ursula Storch, Michael Mederos y Schnitzler, and Thomas Gudermann, 2012. G protein-mediated stretch reception. *American Journal of Physiology-Heart and Circulatory Physiology*, 302:H1241–H1249.

[58] Leonor Michaelis, and Maud L Menten, 1913. Die kinetik der invertinwirkung. *Biochem. z*, 49(333-369):352.

[59] Kimiko Yamamoto, Risa Korenaga, Akira Kamiya, and Joji Ando, 2000. Fluid shear stress activates Ca^{2+} influx into human endothelial cells via P2X4 purinoceptors. *Circulation research*, 87:385–391.

[60] Samira Samtleben, Juliane Jaepel, Caroline Fecher, Thomas Andreska, Markus Rehberg, and Robert Blum. Direct imaging of ER calcium with targeted-esterase induced dye loading (TED). *JoVE (Journal of Visualized Experiments)*, (75):e50317, 2013.

[61] Akitoshi Miyamoto and Katsuhiko Mikoshiba. Probes for manipulating and monitoring IP_3. *Cell Calcium*, 64:57–64, 2017.

[62] Mark J Henderson, Emily S Wires, Kathleen A Trychta, Xiaokang Yan, and Brandon K Harvey. Monitoring endoplasmic reticulum calcium homeostasis using a Gaussia luciferase SERCaMP. *JoVE (Journal of Visualized Experiments)*, (103):e53199, 2015.

[63] Priyavathi Dhandapani, Srujan Kumar Dondapati, Anne Zemella, Dennis Bräuer, Doreen Anja Wüstenhagen, Stefan Mergler, and Stefan Kubick. Targeted esterase-induced dye (TED) loading supports direct calcium imaging in eukaryotic cell-free systems. *RSC advances*, 11(27):16285–16296, 2021.